*Kidney International, Vol. 56 (1999), pp. 92–103*

# Role of fibronectin deposition in cystogenesis of Madin-Darby canine kidney cells

**Si-Tse Jiang, Huei-Ching Chiang, Min-Hsiung Cheng, Tzi-Peng Yang, Woei-Jer Chuang, and Ming-Jer Tang**

*Department of Physiology and Department of Biochemistry, National Cheng Kung University Medical College, Tainan, and Department of Pathology and Department of Anatomy, Chung Shan Medical and Dental College, Taichung, Taiwan*

**Role of fibronectin deposition in cystogenesis of Madin-Darby canine kidney cells.**

*Background.* Madin-Darby canine kidney (MDCK) cells cultured within collagen I gel exhibit clonal growth and form spherical multicellular cysts. The cyst-lining epithelial cells are polarized with the basolateral surface in contact with the collagen gel and the apical surface facing the lumen. To understand whether MDCK cysts construct the basal lamina, we characterized the composition of the extracellular matrix deposited by MDCK cysts. The cyst-lining cells produced an apparently incomplete basal lamina containing a discontinuous laminin substratum. In addition, the basal cell surface of the cyst was surrounded by a thick layer of fibronectin. This study was conducted to delineate the role of fibronectin deposition in cystogenesis.

*Methods.* MDCK cells cultured in collagen gel were employed. We first used Arg-Gly-Asp (RGD) peptides containing disintegrin rhodostomin to disturb the interaction between fibronectin and the cell surface integrin. We then established several stable transfectants expressing the fibronectin antisense RNA and with which to directly examine the role of fibronectin in cystogenesis.

*Results.* Rhodostomin markedly decreased the growth rates of the MDCK cyst, suggesting the importance of a normal interaction between fibronectin and integrins. The stable transfectants overexpressing the fibronectin antisense RNA exhibited relatively lower levels of fibronectin and markedly lower cyst growth rates than the control clone. The lower growth rate was correlated with an increase in collagen gel-induced apoptosis.

*Conclusions.* The results indicate that the deposition of fibronectin underlying the cyst-lining epithelium serves to prevent apoptosis induced by three-dimensional collagen gel cultures, and hence facilitates cyst growth of MDCK cells.

Epithelial cells can form continuous layers in which they become polarized and much less mobile [1]. In single-layered epithelia, apical and basolateral cell surfaces are separated by tight junctions. The basal surface of an epithelial sheet usually rests on a basement membrane that represents a special type of extracellular matrix (ECM), which mainly contains laminin, type IV collagen, entactin, and proteoglycan [2]. Special receptors for laminin and collagen have been localized on the basolateral membranes and thus may function in providing proper interactions for epithelial cells to the ECM [3, 4]. Epithelial basement membranes are constantly required to not only provide support, but also to maintain the structural and functional polarity of epithelium.

The cultured canine kidney epithelial line, Madin-Darby canine kidney (MDCK), retains many of the differentiated characteristics of the distal nephron. This line contains all of the elements of a polarized cell surface and has been extensively used by cell physiologists to study transepithelial transport of water and electrolytes [5]. An individual MDCK cell suspended in type I collagen gel proliferates and forms epithelial cysts, in which a polarity is established with the basolateral surface facing the collagen gel and the apical surface facing the lumen [6]. This MDCK cyst appears to be a convenient *in vitro* model for examining the cellular mechanisms involved in morphogenesis and enlargement of renal cyst and perhaps the pathogenesis of renal cystic disease [7, 8].

Renal cystic diseases include a diverse group of diseases characterized by the formation and growth of fluid-filled epithelial cell-lined sacs within the kidney [9]. Renal cysts may form as a consequence of a hereditary disorder, a developmental abnormality, exposure to a cystogenic chemical, or may be acquired because of unknown reasons. The mechanisms of renal cyst formation and growth are not yet clear, but at least three types of abnormalities are involved: fluid accumulation, alternations in basement membranes, and epithelial cell proliferation. Several studies on humans and experimental forms of polycystic kidney disease (PKD) have demon-

**Key words:** cyst, apoptosis, anti-sense RNA, cell proliferation, collagen, disintegrin, transfection.

Received for publication October 6, 1998
and in revised form January 15, 1999
Accepted for publication February 5, 1999

strated an increase in content of fibronectin, but a normal content of laminin, entactin, and type IV collagen in basement membranes lining cystic tubules [10–12]. The possible role of enhanced fibronectin levels in the pathogenesis of PKD is unclear. In addition, the structural and functional integrity of the basement membranes of MDCK cysts has not yet been thoroughly characterized.

This study was undertaken to determine the composition of ECM underneath the MDCK cysts. From immunocytochemical studies and Western blot analyses we observed that an incomplete sheet of basement membrane substratum, without entactin and intact trimeric laminin, constructed the basal lamina of the cyst-lining epithelial cells. In contrast, fibronectin was present in abundance and was organized into a thick continuous sheath beneath the basal surface of MDCK cysts. To further investigate the role of fibronectin deposition in MDCK cyst formation and growth, we used Arg-Gly-Asp (RGD) peptide, which containes disintegrin or engineered MDCK cells that express fibronectin antisense RNA to block the function or synthesis of fibronectin, respectively. We found that fibronectin deposition is essential for the growth of MDCK cyst. These findings provide a strong *in vitro* evidence for the role of fibronectin in the pathogenesis of PKD.

## METHODS

### Cell culture

Madin-Darby canine kidney cells were maintained in Dulbecco's modified minimal essential medium (DMEM) containing 10% fetal calf serum (FCS) at 37°C in a humidified 5% $CO_2$ atmosphere. A subline, designated Y224, was derived from a single MDCK cyst in collagen gel by the procedure described previously [13]. We used a modified method of McAteer, Evan, and Gardner to culture Y224 cells in type I collagen gel [6]. For cell harvest, the culture medium was removed, and the collagen gel was dissolved with 1 ml of 2 mg/ml collagenase (Worthington, Freehold, NJ, USA) in DMEM at 37°C for 20 minutes. The cysts were detached from the collagen gel and dissociated into single cell suspensions with trypsin/ethylenediaminetetraacetic acid (EDTA). All cell counts were made using a hemocytometer, and viability was determined by trypan blue dye exclusion.

### Antibodies

The following antibodies were used: rabbit antifibronectin, laminin, and vitronectin (Biogenesis, Poole, UK), rat antientactin (Biogenesis). Fluorescein (FITC)-conjugated antirabbit IgG was purchased from Sigma Chemical Co. (St. Louis, MO, USA). Horseradish peroxidase (HRP)-conjugated antirabbit and antirat IgG were purchased from Jackson Immuno Research Lab Inc. (West Grove, PA, USA).

### Western blotting

Cells grown in collagen gel were harvested by incubation with collagenase (2 mg/ml) at 37°C for 20 minutes. The released cells were gently collected by low-speed centrifugation (500 *g* for 3 min), washed twice with phosphate-buffered saline (PBS), and then homogenized by sonication in a buffer containing 50 mM Tris-HCl, pH 7.4, 100 mM NaCl, 1 mM benzamidine hydrochloride, 1 mM EDTA, 20 mM 6-amino-*N*-caproic acid, 2 mM phenylmethylsulfonyl fluoride (PMSF), 0.1% sodium dodecyl sulfate (SDS), and 1% Triton X-100. The homogenate was stored at −80°C prior to analysis.

Protein extract (30 μg) from each sample was resolved by SDS-polyacrylamide gel electrophoresis (SDS-PAGE) and was electrophoretically blotted onto nitrocellulose paper. The nitrocellulose paper was incubated with primary antibody, and immunocomplexes were detected with HRP-conjugated goat antimouse (or antirabbit) IgG antibody (1:10,000 dilution). They were then made visible by fluorography with enhanced chemiluminescence detection kit (ECL; Amersham International, Arlington Heights, IL, USA). The resulting fluorographs were analyzed by a scanning densitometry.

### Immunocytochemical and immunofluorescence staining

The type I collagen gels containing cultured MDCK cysts were removed from the culture dishes, fixed with formalin, embedded in paraffin, sectioned, deparaffinated, and stained with hematoxylin-eosin according to standard histological methods.

For immunohistological staining procedures, the deparaffinated sections were extensively rinsed in PBS. After blocking endogenous peroxidase activity with 0.3% $H_2O_2$ in methanol, the sections were reacted with normal goat serum, followed by a reaction with an appropriately diluted rabbit polyclonal antibody. Next, the sections were washed and reacted with a biotinylated goat antirabbit IgG antibody, followed by streptavidin-conjugated HRP. After further washing, the sections were reacted with 0.05% diaminobenzidine containing 0.01% $H_2O_2$ for color development. The cell nuclei were counterstained with hematoxylin. Finally, the sections were rinsed, dehydrated in a graded ethanol series, and mounted.

For immunofluorescence staining procedures, the deparaffinated sections were rinsed in PBS, and nonspecific binding sites were blocked with normal goat serum, followed by incubation with an appropriately diluted primary antibody. After further rinsing in PBS, samples were incubated in secondary antibodies (goat antirabbit IgG-FITC or goat antimouse IgG-Rhodamine). Samples were rinsed in PBS, mounted in 90% glycerol in PBS,

```
GAGACACCTG CAGCAAGAAG GATAATCGAG GAAACCTGCT CCAGTGCATC TCGACAGGCA   60
ACGGCCGGGG GGACTGCAAG TCTGAGAGGT CGACCTCTCT GCAGACCACT TCCACCGGAT  120
CTGGCCCCTT CACAGATGTC CGGACAGGCA TTTACCAGCC CCAGCCTCAC CCACAGCCGG  180
CTCCCTACCG TCACTGCGTC TCGGACAGTG GCGTGGTTTA CTCTGTGGGG ATACGGTGGC  240
TGAAGACACA AGGAAATAAG CAAATGCTTT GCACTTGCCT GGGCAATGGA ATCTGCTGCC  300
AAGAAACAGC CGTCACCCGA ACTTACGGTG GCAATTCAAA CGGGGAACCC TGTGTCTTAC  360
CATTCACCTA CAACGGCAGG ACTTTCTACT CCTGCACCAC AGAAAGGCGG CAGGATGGAC  420
ATCTGTGGTG CAGCACAACT TCCAATTACG AACAAGACCA GAAGTTCTCC TTCTGTACAG  480
ACCATACTGT TTTGGTTCAG ACTCGAAGTG GAAATTCCAA TGGTGCCTTG TGCCACTTCC  540
CTTTCCTGTT CAACAACCAC AACTACACGG ACTGTACTTC TGAGGGCAGG AGAGACAACA  600
TGAAGTGGTG CGGAACCACG CCGAATTAGG ATGCTGACCA GAAGTTTGGA TTTTGCCCCA  660
TGGCCGCCCA TGAGGAAATC TGCACAACCA ATGAAGGGGT CATGTATCGC ATTGGAGATC  720
AGTGGGACAA ACAGCACGAT ATGGGCCACA TGATGAGGTG CACATGCGTT GGGAATGGTC  780
GTCGAGAATG GACTTGTGTT GCCTACTCCC AGCTCCGAGA TCAGTGCATT GTTGATGACA  840
TCACTTACAA TGTGAACGAC ACATTCCACA AGCGTCATGA AGAGGGACAC ATGCTGAATT  900
GTACTCGCTT TGGTCAGGGC CGGGGCAGAT GGAAGTGCGA TCCCATTGAC CAATGCCAGA  960
ATTCAGAGAC TG                                                      972
```

**Fig. 1. The cDNA sequence of canine fibronectin.** The 972 bp segment of canine fibronectin cDNA was synthesized by the method described in the **Methods** section. This sequence is approximately 89% homologous with corresponding human fibronectin cDNA.

observed with a Zeiss microscope with epifluorescence, and photographed in an LSM-40 laser-scanning confocal imaging system.

### Rhodostomin expression and purification

The rhodostomin gene, kindly provided by Dr. S.J. Lo, was cloned and expressed in the *E. coli* system [14]. The engineered strain of BL21 carries vector pGEX-2KS for GST-Rhodostomin. The expression of GST-Rhodostomin and its D51E mutant protein was induced by the addition of isopropylthiogalactoside (IPTG) and purified by glutathione S transferase affinity chromatography (Pharmacia Biotech, Uppsala, Sweden). From the SDS-PAGE analysis, both rhodostomin and its D51E mutant protein were found to be homogenous.

### Reverse transcription-polymerase chain reaction, DNA sequencing, and plasmid construction

Total RNA was isolated from cultured MDCK cells by the standard guanidium isothiocyanate extraction method. Reverse transcription (RT) and polymerase chain reaction (PCR) were performed using a kit (RNA Amp; Perkin Elmer, Norwalk, CT, USA). Primers used to amplify a 972 bp segment of canine fibronectin cDNA were as follows: sense primer 5′-GAGACACCTGCAG CAAGAAGGATAATC-3′ (nucleotides 648 to 674 in human fibronectin cDNA) and antisense primer 5′-CAGT CTCTGAATTCTGGCATTGGTC-3′ (nucleotides 1595 to 1619 in human fibronectin cDNA) [15]. The amplification conditions were as follows: first 95°C for two minutes, then 35 cycles of 95°C for one minute, 65°C for one minute, and a final extension at 72°C for seven minutes. The 972 bp PCR product was purified from 0.8% agarose, cleaved with Pst I and EcoR I, and ligated into pBS (Stratagene, La Jolla, CA, USA) to create pBSFN, which was finally transfected into *E. coli.* The sequences of canine FN cDNA analyzed by the ABI Prism 377 automated sequencer using T3 or T7 primers are shown in Figure 1. The canine fibronectin sequence is approximately 89% homologous with the human fibronectin cDNA.

The Pst I cohesive ends of fibronectin cDNA were converted to BamH I ends with BamH I-Pst I adaptors (BioLabs, Hitchen, Hertfordshire, UK). The converted cDNA containing BamH I and EcoR I overhangs at the 5′ and 3′ ends was ligated into pSG5 (Stratagene) in an antisense fashion to create pSG5FN.

### Transfection and clonal selection

The pSG5FN and ptk*neo* plasmid DNA were cotransfected into MDCK cells by the method of lipofection.

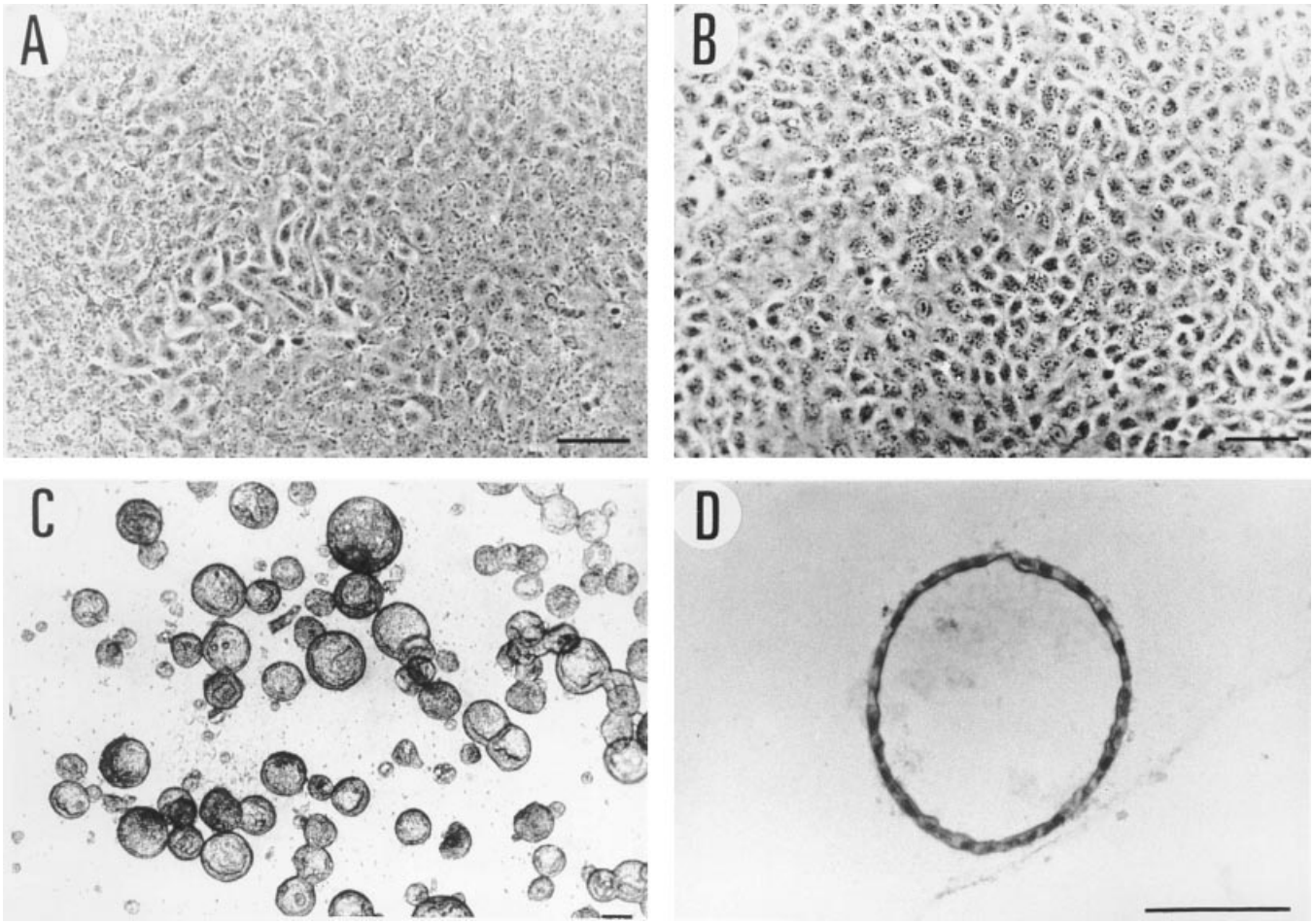


**Fig. 2. Morphology of MDCK and Y224 cells cultured in various conditions.** (*A*) A confluent monolayer culture of parental MDCK cells on a plastic plate shows a heterogeneous morphology (phase contrast microscopy). (*B*) The monolayer culture of Y224 cells on a plastic plate is composed of apparently homogeneous polygonal cells. (*C*) Cystic colony formed by Y224 cells cultured for eight days in collagen gel (phase contrast microscopy). (*D*) Hematoxylin-eosin stained picture of Y224 cyst-lining epithelial cells (light microscopy). Bar indicates 100 μm.

At 40 to 70% confluence, cells were transfected with 5 μg/ml plasmid DNA (4.9 μg/ml of pSG5FN and 0.1 μg/ml of ptk*neo*) mixed with 35 μl/ml LipofectAMINE (GIBCO BRL, Grand Island, NY, USA) in Opti-MEM–reduced serum media (GIBCO BRL) according to the manufacturer's instructions for transfection of adherent cells. In addition, pSG5 plasmid and ptk*neo* were also cotransfected into cells as a control. After 24 hours, the medium was replaced with DMEM containing 10% FCS and incubated for another 24 hours. Subsequently, the cells were trypsinized and replated in a standard culture medium containing 500 μg/ml of G418. After three weeks, G418-resistant cells were trypsinized and cloned using the limited dilution method.

### Northern blot hybridization

The method for Northern blot analysis has been described previously [13]. The specific mRNA immobilized on nitrocellulose filter was detected by hybridizing with canine fibronectin cDNA probe, which had been radiolabeled with $^{32}P$ by a random primer-labeling method.

### Analysis for apoptosis

Cells grown in collagen gel were washed twice with PBS and released from the gels by incubation with collagenase (2 mg/ml) at 37°C for 20 minutes. The released cells were dissociated into single-cell suspensions with trypsin/EDTA. After being washed twice with PBS, the cells were fixed with 70% ethanol, treated with ribonuclease [RNase; 100 μg RNase/ml Tris + EDTA (TE)], and stained with propidium iodine (40 μg/ml PBS). Finally, the cells were incubated in the dark at room temperature for 30 minutes and analyzed by flow cytometry using a FACScan (Becton-Dickinson, Mountain View, CA, USA) with excitation set at 488 nm. Data were analyzed by a cell-fit software program and represented as histographs and numbers. For extraction of low molecular genomic DNA, cell pellets were resuspended and

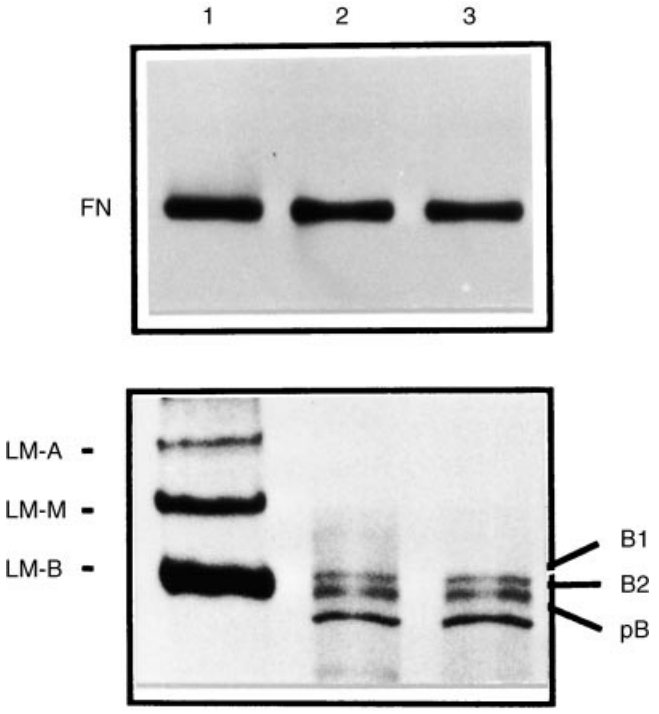


**Fig. 3. Detection of fibronectin and laminin in MDCK cells by Western blot.** Cell extracts were prepared from cells cultured in collagen gel for six (lane 2) and eight (lane 3) days. Lane 1 indicates purified fibronectin (FN) and laminin (LM) isolated from human plasma and placenta, respectively, as positive controls. In MDCK cells, two laminin B chains (B1 and B2) and one premature laminin B chain (pB) are present. The laminin A chain is absent in these cultures. The positions of laminin A, B, and M chains of human placenta laminin (LM-A, LM-B, and LM-M) are also indicated.

lyzed with extraction buffer (0.5% Triton X-100, 10 mM EDTA, and 10 mM Tris-HCl, pH 8). Samples were then extracted twice with phenol/chloroform and DNA precipitated with isopropanol. DNA was recovered by centrifugation and washed with 75% ethanol, air dried, and resuspended in 20 μl TE with 20 μg/ml RNase A. Samples were then incubated at 37°C for one hour. DNA samples were then electrophoresed on a 1.5% agarose gel in Tris-borate/EDTA (TBE) buffer. Finally, the DNA was briefly stained with ethidium bromide and visualized under ultraviolet light.

## RESULTS

The Y224 cells derived from a single MDCK cyst were used in these experiments. This line exhibits a homogeneously polygonal morphology in confluent monolayer culture when compared with the original MDCK cell line (Fig. 2 A, B). After 6 to 10 days in culture, Y224 cells in collagen gel formed multicellular cysts in spherical structures (Fig. 2 C, D). The composition of ECM produced by MDCK cyst-lining cells was determined by assessing the levels of entactin, fibronectin, laminin, and vitronectin with Western blotting. As shown in Figure 3, two laminin B chains and a premature form of laminin B chain (pB) were observed. However, laminin A chain was almost absent, suggesting that MDCK cysts did not synthesize a trimeric and mature laminin comprising one A subunit and two B subunits (B1 and B2). Although defective, the laminin was still present as a dotted irregular pattern on the basal surface of MDCK cysts when the cysts were fixed with formaldehyde at day 8 and examined by immunohistochemistry (Fig. 4 E, F). Because laminin is a major component of the epithelial basement membranes, lacking laminin deposition in the basal surface would make poorly organized epithelial basement membranes. In addition, entactin and vitronectin, as judged by Western blot, were almost absent in MDCK cysts (data not shown).

In contrast, the contents of fibronectin were abundant during cyst formation (Fig. 3) and were strongly stained along the basal surface of MDCK cysts in a continuous pattern, no matter that it was assayed by immunoperoxidase or immunofluorescence-labeling methods (Fig. 4 A–D). It appears as a thick homogenous structure lying immediately below the basal surface of the epithelial cells. Because fibronectin is a major component of the extracellular matrices and is also present in the body fluid including serum, we were suspicious about whether the fibronectin observed on MDCK cysts came from FCS. We therefore seeded the cells in collagen gels supplied with serum-free medium. The cysts formed were a bit smaller, but they all exhibited a thick layer of fibronectin underlying the basal surface of cyst-lining cells (data not shown). These results indicate that cystic-lining epithelial cells could synthesize and deposit fibronectin during cyst formation.

In addition to Y224 cells, we also isolated three other MDCK sublines, each derived from a single cyst. The fibronectin contents of these MDCK sublines were assessed by Western blot analysis (Fig. 5A). Among these cell lines, Y224 exhibited the highest levels of fibronectin. Interestingly, Y224 cells also developed epithelial cyst growth most vigorously in collagen gel (Fig. 5 B–E). These data indicate that the fibronectin levels correlate with the epithelial cyst enlargement.

To study the possible role of fibronectin in renal cyst formation and growth, we used synthetic rhodostomin to disrupt the interaction between fibronectin and its receptor. The RGD peptide containing rhodostomin, acting as a disintegrin, inhibited cyst growth in a dose-dependent manner (Fig. 6). In a negative control experiment in which RGD in rhodostomin was substituted by arginine-glycine-glutamate (RGE), little growth inhibition was observed. These results support the possibility that fibronectin might facilitate MDCK cyst growth.

We therefore assessed the direct involvement of fibronectin in cystogenesis by inhibiting the endogenous

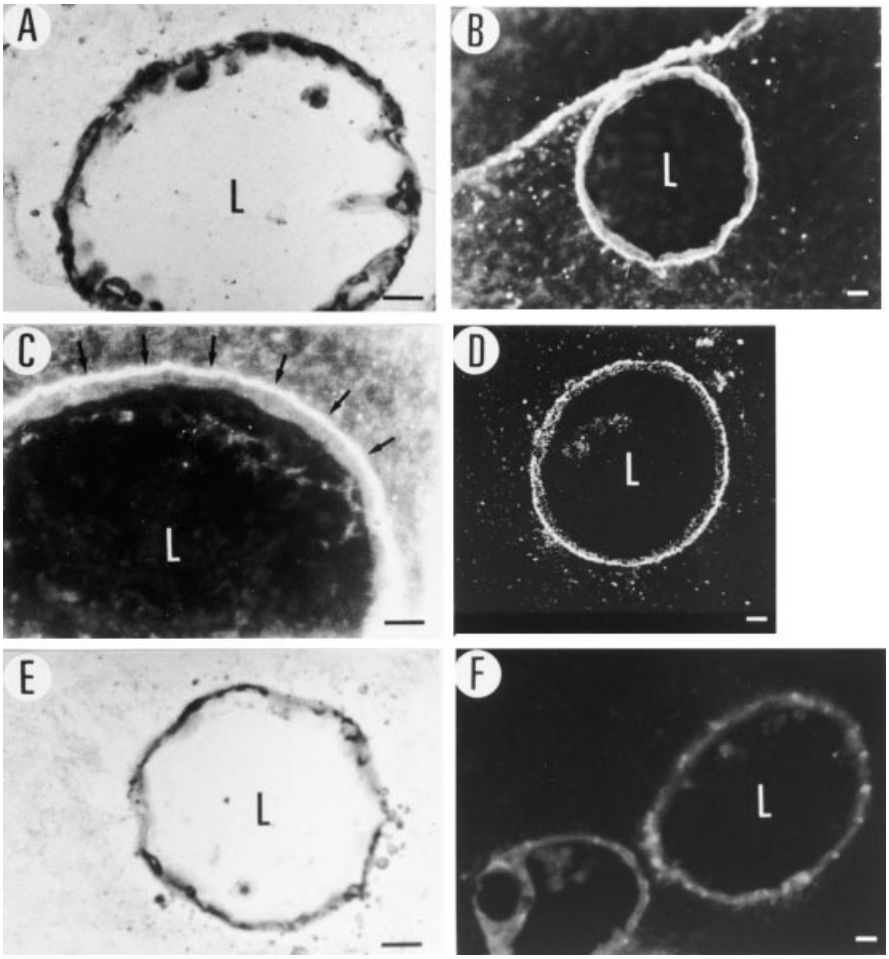


**Fig. 4. Immunolocalization of fibronectin and laminin in Y224 cysts.** Sections were stained by immunoperoxidase (*A, E*) or the immunofluorescence (*B, C, D, F*) method using antibody against fibronectin (A–D) or laminin (E, F). All of these sections were observed by light microscopy (A, E), fluorescence microscopy (B, C, F), or confocal laser scanning microscopy (D). The cystic lumen (L) is indicated in all photographs. Fibronectin is localized mainly under the basal surface of cyst-lining epithelial cells (arrows) and forms a thick layer sheath between cyst lining cells and collagen (scale bar, 20 μm).

synthesis of fibronectin to see if the cyst formation was affected. Y224 cells were stably transfected with a plasmid pSG5FN that had been constructed with an antisense sequence of canine fibronectin mRNA as described in the **Methods** section. The expression of fibronectin in most G418-resistant clones was affected by the antisense RNA construct to various extents. Transfectant clone 6 (pSG5FN#6) expressed the lowest levels of fibronectin in these antisense transfectants, whereas clones 2 and 4 expressed intermediate levels, as demonstrated by the Western blot (Fig. 7A). Densitometric scanning of the blots revealed a 65, 45, or 35% decrease in fibronectin contents for clones 6, 2, or 4, respectively. The protein contents of laminin B chain were not affected by the antisense expression, suggesting that the fibronectin expression was specifically suppressed by the antisense construct. Northern blot analysis of fibronectin mRNA expression revealed a marked decrease in the fibronectin transcript in transfectant clone pSG5FN#6 and a moderate decrease in clones 2 and 4 (Fig. 7B), compatible with the finding of Western blot.

These antisense and control clones were then cultured in collagen gels to determine the association of fibronectin levels with cyst growth. As expected, the control clone with plasmid pGS5 exhibited the same cyst structure as the parental Y224 cells (Fig. 8). In contrast, all of these antisense clones grew slowly and formed relatively smaller cysts than the control clone (Fig. 8). Among the transfectants, clone 6 exhibited the lowest cystic growth rate, in parallel to the fibronectin content of these antisense clones. These data strongly suggest that the accumulation and deposition of fibronectin does facilitate cyst growth and enlargement.

In our previous work, we found that massive apoptotic bodies were present both inside and outside of MDCK cysts in collagen gel culture [16]. Because the growth of cells in cultures is a summarized result of cell proliferation and death, we assessed whether the attenuation in cyst growth by the antisense expression could result from an increase in apoptosis. To test this possibility, all of these transfectants cultured in collagen gels were collected separately on day 8, and their low molecular DNA

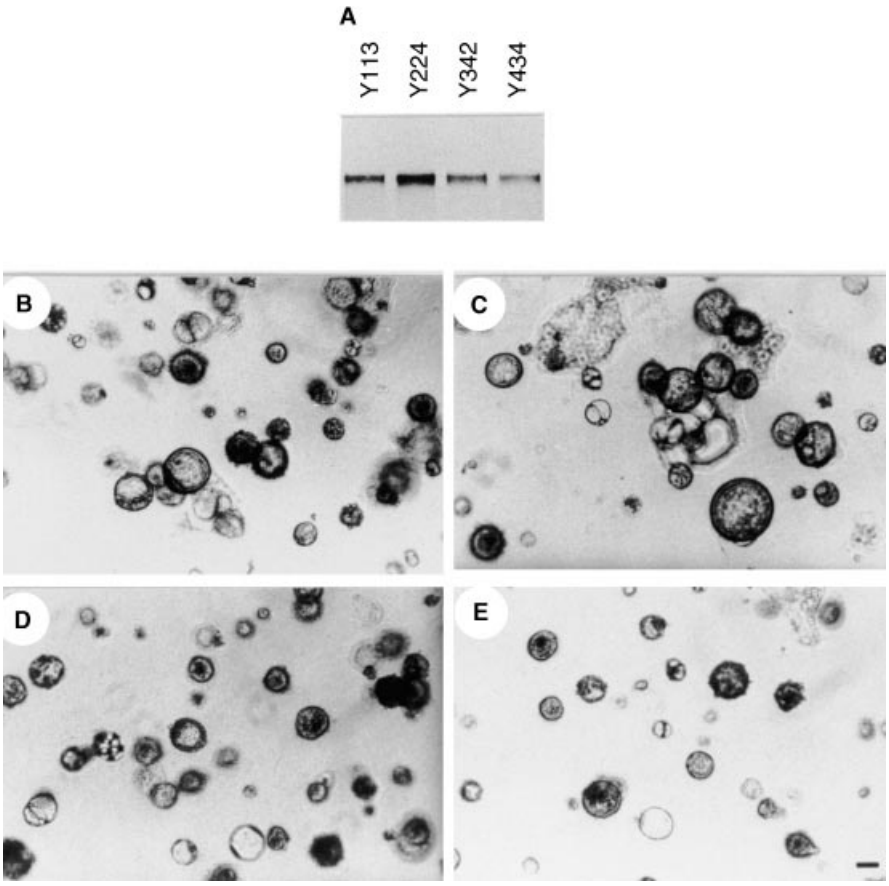


**Fig. 5. Fibronectin contents (*A*) and cyst growth (*B–E*) of various MDCK sublines.** Fibronectin levels were assessed by Western blot analysis. Cell extracts were prepared from various sublines cells cultured on plastic plates for two days. (B–E) shows the cystic morphology of MDCK sublines Y113 (B), Y224 (C), Y342 (D), and Y434 (E) cells cultured in collagen gels for eight days. Y224 cells exhibit the largest cyst size as well as highest fibronectin levels.

was extracted and resolved by electrophoresis. The DNA ladder (Fig. 9A) is apparent in all of these transfectants, and an increase in the intensity of DNA ladder is also obvious in FN antisense transfectants (Fig. 9A). To quantitate the ratio of apoptosis in these cultures, we analyzed the size of nuclei stained with propidium iodide by the flow cytometry. The sub-G0/G1 phase of the cell cycle is evaluated as cell populations containing apoptosis [16]. As shown in Figure 9B, the apoptotic ratio in the control cell population is only 21% and is increased to approximately 33 and 30% in transfectants 2 and 4 possessing antisense pSG5FN, respectively. Transfectant 6 exhibits the highest fraction of apoptosis, being as high as 41%. Taken together, the apoptotic ratio seems to be inversely proportional with the fibronectin content in cyst-lining epithelial cells. We propose that the fibronectin deposited by MDCK cyst functions as a survival factor through the suppression of apoptosis induced by three-dimensional collagen gel cultures, and results in augmented cyst growth and enlargement.

## DISCUSSION

We have used an *in vitro* model to demonstrate the role of fibronectin deposition in the cystogenesis of MDCK cells. Because MDCK cells obtained from American Type and Culture Collection (Rockville, MD, USA) were heterogeneous in morphology, we subcultured the cells and obtained a clone, Y224, from a single cyst. The patterns of fibronectin deposition as revealed by immunohistochemistry were the same in Y224 cells as in the parental MDCK cells. Furthermore, disintegrin inhibits cyst growth to the same extent in Y224 cells as in the parental MDCK cells (data not shown), suggesting that the phenomena observed in these studies are general for MDCK cystogenesis, and not only specific to the Y224 cells.

Fibronectin is a group of closely similar proteins (20 possible variants in humans) generated by alternative splicing from a premRNA, which is transcribed from a single gene. Fibronectin exists in two major forms: soluble dimers and insoluble fibrillar networks. They are first synthesized as soluble dimers that are then polymerized into fibrils. The fibronectin locating on the basal surface of MDCK cysts could be the fibrillar form because MDCK cysts released by collagenase from collagen gels still display this fibronectin layer underlying their basal surfaces. The accumulation and deposition of fibronectin beneath the basal sites of renal epithelial cells appear in

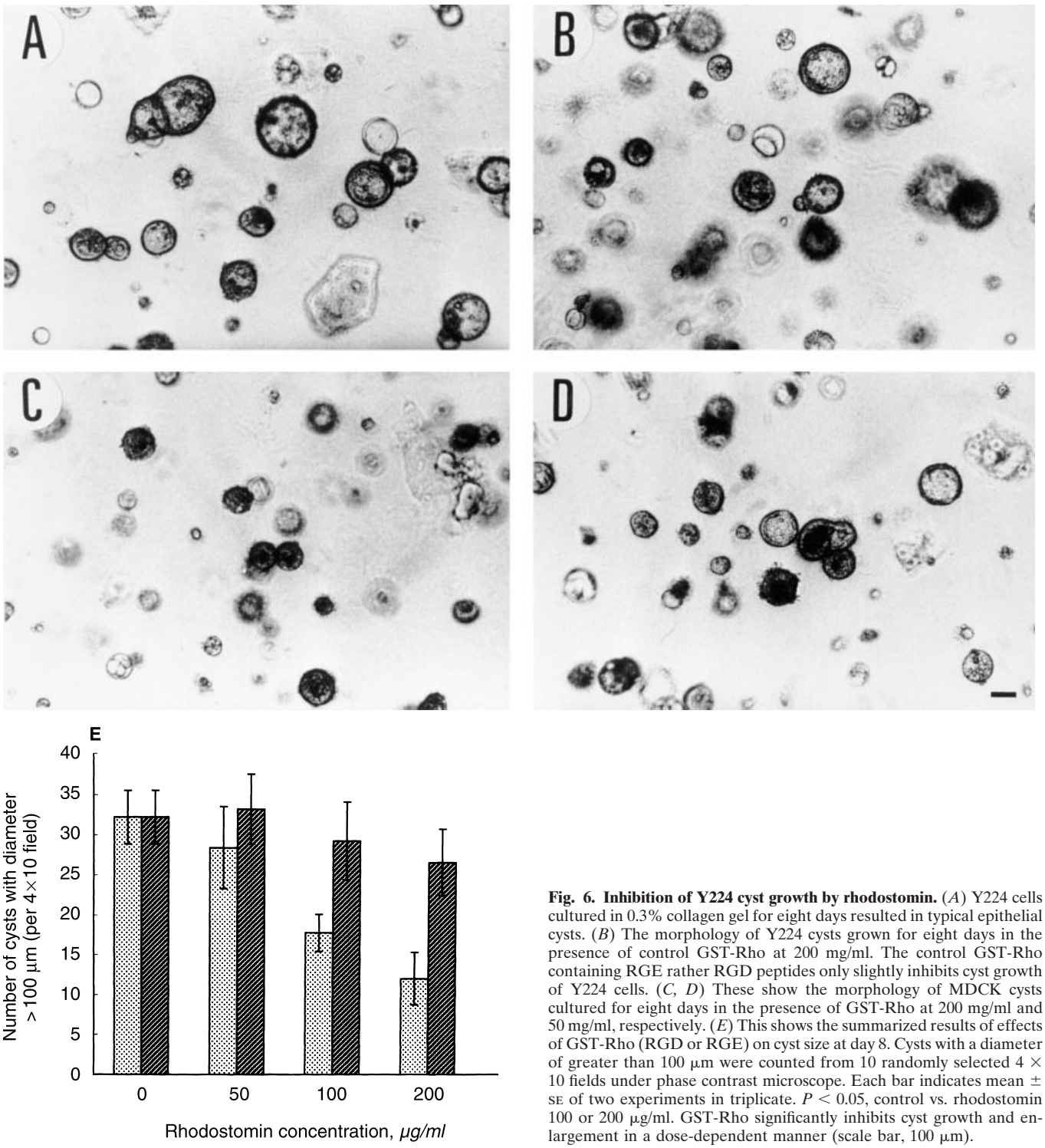


**Fig. 6. Inhibition of Y224 cyst growth by rhodostomin.** (*A*) Y224 cells cultured in 0.3% collagen gel for eight days resulted in typical epithelial cysts. (*B*) The morphology of Y224 cysts grown for eight days in the presence of control GST-Rho at 200 mg/ml. The control GST-Rho containing RGE rather RGD peptides only slightly inhibits cyst growth of Y224 cells. (*C, D*) These show the morphology of MDCK cysts cultured for eight days in the presence of GST-Rho at 200 mg/ml and 50 mg/ml, respectively. (*E*) This shows the summarized results of effects of GST-Rho (RGD or RGE) on cyst size at day 8. Cysts with a diameter of greater than 100 μm were counted from 10 randomly selected 4 × 10 fields under phase contrast microscope. Each bar indicates mean ± SE of two experiments in triplicate. $P < 0.05$, control vs. rhodostomin 100 or 200 μg/ml. GST-Rho significantly inhibits cyst growth and enlargement in a dose-dependent manner (scale bar, 100 μm).

only MDCK cyst-lining cells. However, fibronectin is almost absent in the fully confluent MDCK cell monolayers cultured on collagen gels (unpublished data). Currently, there is limited information in the literature concerning fibronectin fibril assembly by kidney epithelial cells. The fibronectin deposition could be an uncommon behavior in normal renal epithelial cells or could occur only in pathological conditions such as the PKD. The issue concerning the process of fibronectin fibril assembly is very important and is still under investigation. Here, we provide an ideal *in vitro* model to study this topic.

Basement membrane that contains extracellular matri-

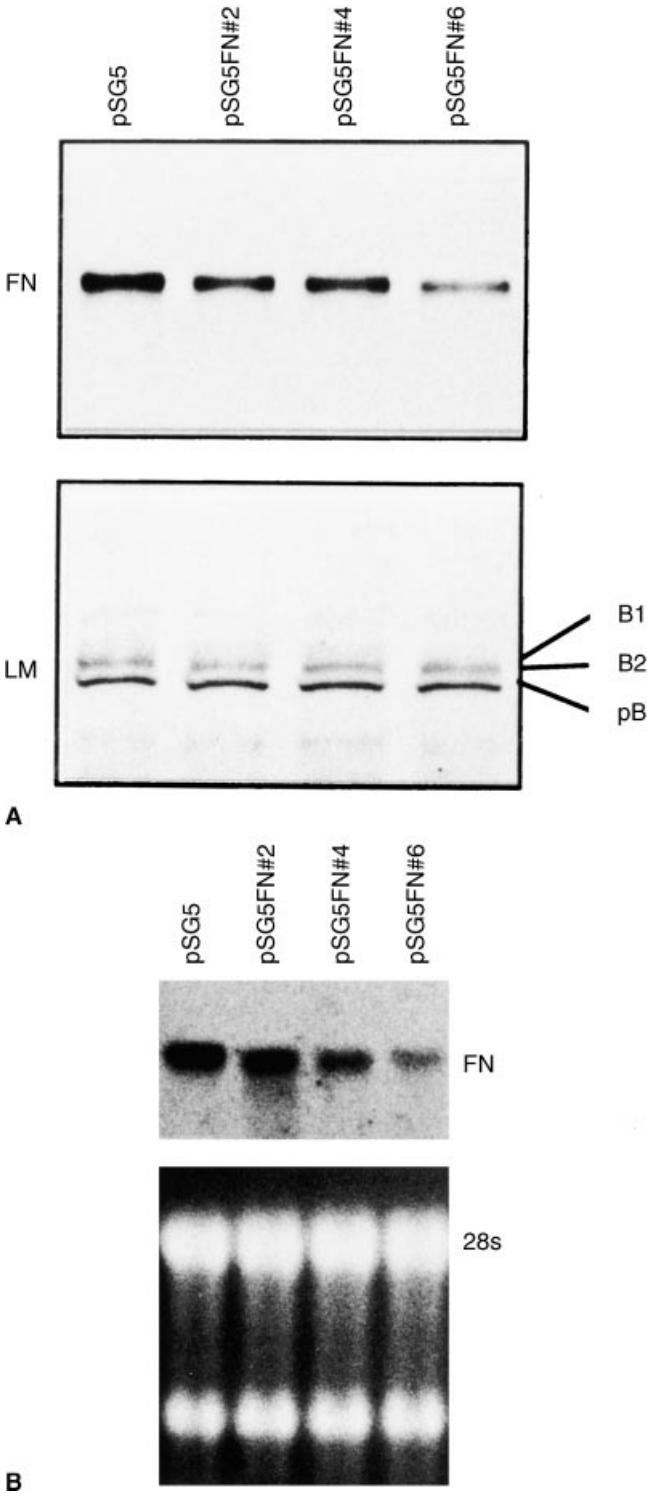


**Fig. 7. Expression of fibronectin protein (*A*) and mRNA (*B*) in various transfectants harboring fibronectin antisense RNA.** (A) Western blot analysis of fibronectin (FN) and laminin (LM) in control cells (pSG5) and various transfectants (pSG5FN). The position of two laminin B chains (B1 and B2) and one premature laminin B chain (pB) is also indicated. These transfectants contain equal amounts of laminin B chains, but their fibronectin levels are down-regulated to various degree, indicating that transfection has been successfully achieved. (B) Northern blot analysis to detect fibronectin mRNA levels in control cells and various transfectants. The ribosomal RNA is also shown.

ces plays very important roles in the development of epithelial tissue. Laminin, in particular, has been proposed to be directly responsible for eliciting many of the biological responses of the epithelium to the basement membrane because it has many activities *in vitro* [17, 18]. These effects are mediated by laminin receptor [19]. In MDCK cysts, the laminin A chain is almost absent, and the deposition of laminin is no more a continuous pattern along the basal surface than it is in normal epithelia. In fact, MDCK cysts examined by routine transmission electron microscopy appear to lack a well-organized continuous basal lamina [6]. The extracellular materials of MDCK cysts accumulate, instead, in irregular patches. The fixation in the presence of ruthenium red demonstrated abundant flocculent electron-dense material associated with basement membrane [6]. Our observations suggest that these loosely composed extracellular materials are likely to be constructed mainly by fibronectin, and hence, the morphology of cystic basement membrane is different from the normal epithelial basal lamina. Nevertheless, cells of MDCK cysts are polarized to form a true luminal and basolateral surface [6]. These results indicate that the maintenance of the polarity of MDCK cysts does not require normal epithelial basal lamina. Likewise, MDCK cells cultured on nitrocellulose filters also form polarized epithelial sheets without basal lamina [20]. Taken together, cells of MDCK cysts might be an abnormally differentiated renal epithelium, which exhibits abnormal synthesis and assembly of the ECM. This phenomenon is reminiscent of PKD, in which renal epithelial cells also exhibit defective synthesis of tubular basement membranes.

Renal cyst is the central pathological feature of a number of human congenital and acquired diseases. PKD, the most common human genetically transmitted disease, occurs either in a recessive infantile form (ARPKD) or an autosomal dominant adult form (ADPKD) affecting over 500,000 individuals in the United States, and is responsible for 8 to 10% of all patients receiving dialysis or transplantation for end-stage renal disease [21, 22]. ARPKD typically affects 1 in 10,000 live births, and ADPKD affects up to 1 in 500 individuals in the population [22]. In the past few years, *PKD1* and *PKD2* have been identified as the mutated genes responsible for more than 95% of ADPKD. The products of *PKD1* and *PKD2* genes have been named polycystin 1 and 2. These genes function together as part of a multicomponent membrane-spanning complex involving in the cell–cell or cell–matrix interactions in their extracellular compartment [23]. Structural and biochemical changes in the basement membrane have been described in human PKD [11, 24]. Fibronectin is normally absent in renal tubules, but its contents are increased dramatically in the peritubular regions of cystic segments of the renal tubules. It is very interesting to note that the constituent

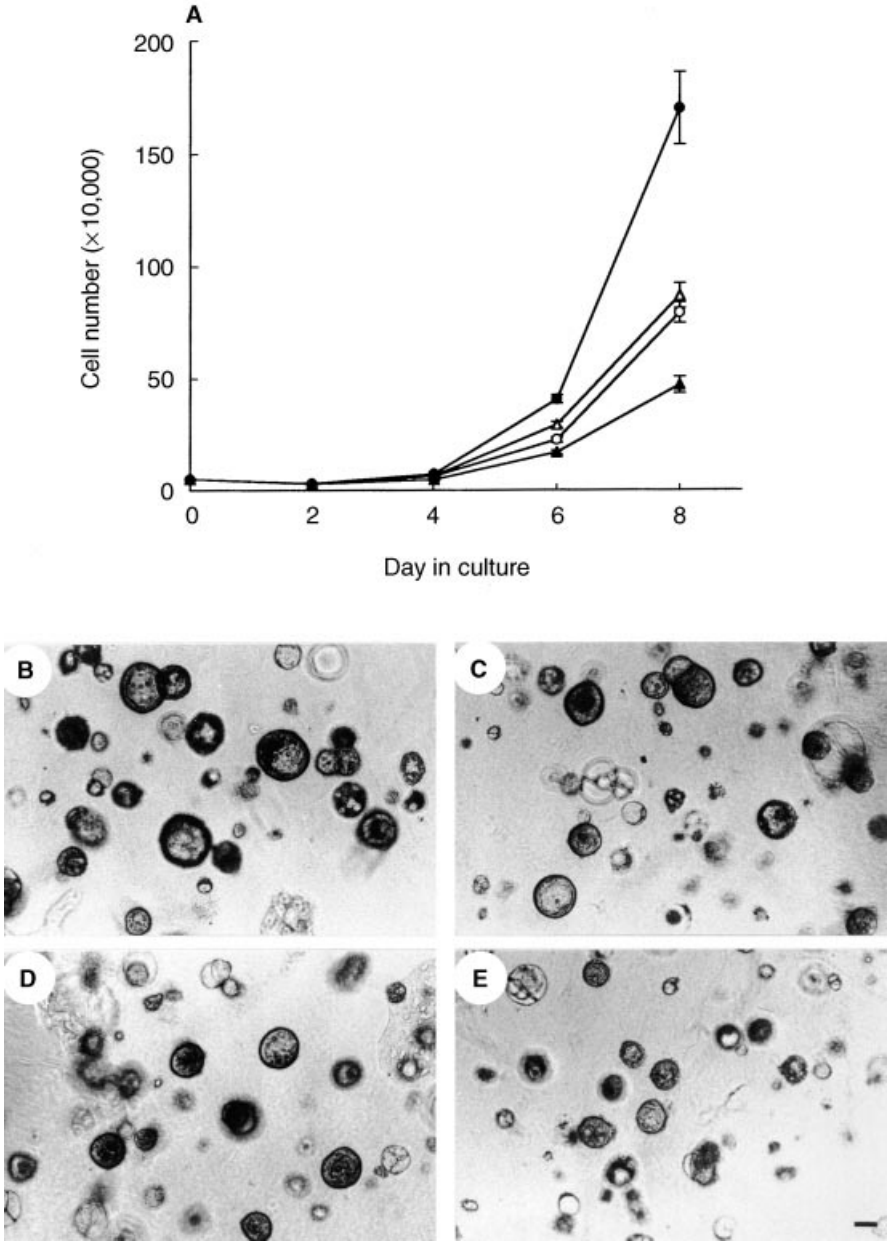


**Fig. 8. Comparison of the cyst growth rates in various fibronectin antisense transfectants.** (*A*) Growth curves of pSG5 control cells (●), antisense expressing pSG5FN#2 (○), #4 (△), and #6 (▲) cells cultured in collagen gel. (*B–F*) depicts cystogenesis of pSG5 control cells (B), pSG5FN#2 (C), #4 (D), and #6 (E) cells cultured in 0.3% collagen gel for eight days. (F) This shows the summarized results of effects of fibronectin antisense RNA on cyst size at day 8. Cysts with diameter greater than 100 μm were counted from 10 randomly selected 4 × 10 fields under phase contrast microscope. Each bar indicates mean ± SE of three experiments in triplicate. $P < 0.05$, control vs. all pSG5FN transfectants. The fibronectin antisense RNA transfectants exhibited markedly slower growth rates in collagen gel than control cells (scale bar indicates 100 μm).

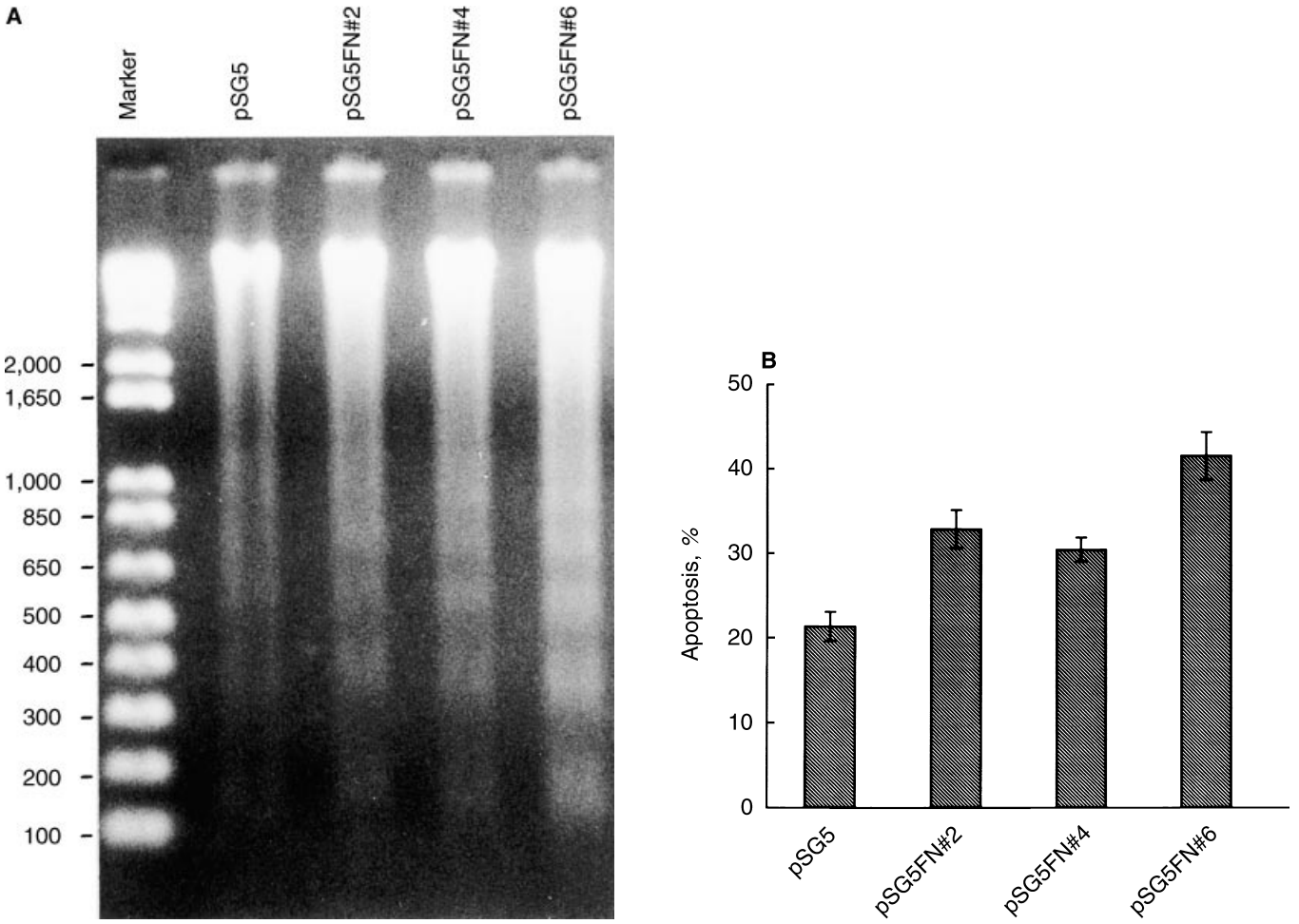


**Fig. 9. Demonstration of DNA fragmentation and comparison of apoptotic ratio in various transfectants cultured in collagen gel.** Cells cultured in collagen gels for eight days were collected, and their low molecular weight DNA was extracted and resolved by electrophoresis. (*A*) This shows the result of DNA ladder in various transfectants. (*B*) This depicts the apoptotic ratio of various transfectants cultured in collagen gel for eight days. FACScan analysis of cell cycle was used and the sub-G0 phase indicates apoptosis population. Each bar indicates mean ± SE of three experiments in duplicate. $P < 0.05$, control vs. all pSG5FN transfectants. The fibronectin antisense transfectants exhibit relatively higher apoptotic ratio in collagen gel cultures than control cells.

changes in the polycystic kidney basement membranes, especially the presence of a thick layer of fibronectin underlying renal cysts, are somewhat similar to those of MDCK cysts cultured in collagen gels. From these studies, we are tempted to propose that fibronectin plays a crucial role in the pathogenesis of PKDs as well as in the cystogenesis of MDCK cells.

We have previously shown that massive apoptotic bodies are present both inside and outside of MDCK cysts in collagen gel culture [16]. Frisch and Francis demonstrated that the disruption of interactions with ECM resulted in apoptosis of the epithelial cell, the so-called homeless cell death [25]. In addition, our laboratory has discovered that epithelial cells may develop apoptosis upon collagen gel overlay [26]. Both studies provide insights into understanding what causes apoptosis of MDCK cells in collagen gel. The study reported here demonstrates that fibronectin is the major component of the ECM produced by cultured MDCK cysts. In addition, subconfluent MDCK cells cultured on plastic plates also synthesize a large amount of fibronectin. However, type I collagen-, fibronectin-, or laminin-coated plates all do not alter the growth rate or morphology of cultured MDCK cells (data not shown). These data suggest that exogenous ECM is not required for the growth of MDCK cells on a normal two-dimensional plate. Nevertheless, MDCK cells may use endogenous fibronectin to facilitate attachment, spreading, growth, and differentiation of themselves in three-dimensional cultures. Recently, exogenous fibronectin has been shown to suppress apoptosis in some attached cells through an integrin-dependent mechanism [27–29]. In this study, we assess the role of endogenous fibronectin in the survival of MDCK cells. This is the first time to demonstrate that the endogenous

fibronectin functions as a survival factor. Fibronectin may support the survival of MDCK cells cultured in collagen gel by transmitting a survival signal via adhesion receptors such as integrins and/or by maintaining the overall structural integrity of the ECM. In the MDCK cyst, it should be of importance to identify which integrins are responsible for the adhesion to fibronectin. It has been established that fibronectin contains an RGD sequence that can be recognized by the extracellular domains of the integrins [30]. In our study, rhodostomin inhibits cyst growth possibly via disrupting the interaction between fibronectin and integrin. Previously, Saleman, Santoro, and Keely observed that inhibition of $\alpha_2\beta_1$ integrin expression or function induced by antisense oligonucleotides or antibodies resulted in increased apoptosis and reduced cyst growth by MDCK cells *in vitro* [31]. However, $\alpha_2\beta_1$ integrin is the major receptor for collagen and laminin but not fibronectin in MDCK cells. MDCK cells also express $\alpha_3\beta_1$, $\alpha_v\beta_3$, and unidentified $\alpha_x\beta_1$ integrins, all of which could possibly serve as fibronectin receptors [32]. It is therefore necessary to clarify which integrins are responsible for transmitting survival and growth signals provided by fibronectin during cyst formation. Taken together, the correlation between polycystins, fibronectin, and integrins is worthy of further investigation.

## ACKNOWLEDGMENTS

This work was supported by DOH88-HR-724 from National Health Research Institute, Taiwan, R.O.C. to M.-J. Tang. We thank Dr. Eric I.-C. Li for helpful suggestions on the manuscript and Ms. Tzi-Ling Chen for excellent technical support.

*Reprint requests to Ming-Jer Tang, M.D., Ph.D., Department of Physiology, National Cheng Kung University Medical College, 1 University Road, Tainan, Taiwan 70101.*
*E-mail: mjtang1@mail.ncku.edu.tw*

## REFERENCES

1. Rodriguez-Boulan E, Nelson WJ: Morphogenesis of the polarized epithelial cell phenotype. *Science* 245:718–725, 1989
2. Timpl R: Structure and biological activity of basement membrane proteins. *Eur J Biochem* 180:487–502, 1989
3. Mecham RP: Laminin receptors. *Annu Rev Cell Biol* 7:71–91, 1991
4. Ekblom P: Renal development, in *The Kidney: Physiology and Pathophysiology*, edited by Seldin DW, Giebish G, New York, Raven Press, 1992, pp 475–501
5. Simons K, Fuller SD: Cell surface polarity in epithelia. *Annu Rev Cell Biol* 1:243–288, 1985
6. McAteer JA, Evan AP, Gardner KD: Morphogenetic clonal growth of kidney epithelial cell line MDCK. *Anat Rec* 217:229–239, 1987
7. Grantham JJ: Fluid secretion, cellular proliferation, and the pathogenesis of renal epithelial cysts. *J Am Soc Nephrol* 3:1843–1857, 1993
8. Tanner GA, McQuillan PF, Maxwell MR, Keck JK, McAteer JA: An in vitro test of the cell stretch-proliferation hypothesis of the renal cyst enlargement. *J Am Soc Nephrol* 6:1230–1241, 1995
9. Welling LW, Grantham JJ: Cystic and develpoment diseases of the kidney, in *The Kidney*, edited by Brenner BM, Rector FC, Philadelphia, W.B. Saunders, 1991, pp 1657–1694
10. Butkowski RJ, Carone FA, Grantham JJ, Hudson GB: Tubular basement membrane changes in 2-amino-4,5-diphenylthiazole-induced polycystic disease. *Kidney Int* 28:744–751, 1985
11. Carone FA, Makino H, Kanwar YS: Basement membrane antigens in renal polycystic disease. *Am J Pathol* 130:466–471, 1988
12. Carone FA, Bacallao R, Kanwar YS: Biology of polycystic kidney disease. *Lab Invest* 70:437–448, 1994
13. Lin HH, Yang TP, Jiang ST, Liu HS, Tang MJ: Inducible expression of *bcl-2* by *lac* operator/repressor system in MDCK cells. *Am J Physiol* 273:F300–F306, 1997
14. Chang HH, Hu ST, Huang TF, Chen SH, Wu-Lee YH, Lo S: Rhodostomin, an RGD-containing peptide expressed from a synthetic gene in *Escherichia coli*, facilitates the attachment of human hepatoma cells. *Biochem Biophys Res Commun* 190:242–249, 1993
15. Kornblihtt AR, Umezawa K, Vibe-Pedersen K, Baralle FE: Primary structure of human fibronectin: Differential splicing may generate at least 10 polypeptides from a single gene. *EMBO J* 4:1755–1759, 1985
16. Lin HH, Yang TP, Jiang ST, Yang HY, Tang MJ: Bcl-2 overexpression prevents apoptosis-induced MDCK simple epithelial cyst. *Kidney Int* 55:168–179, 1999
17. Beck K, Hunter I, Engel J: Structure and function of laminin: Anatomy of a multidomain glycoprotein. *FASEB J* 4:3148–3160, 1990
18. Klein G, Langegger M, Timpl R, Ekblom P: Role of laminin a chain in the development of epithelial cell polarity. *Cell* 55:331–341, 1988
19. Graf J, Iwamoto Y, Sasaki M, Martin GR, Kleiman HJ, Robey FA, Yamada Y: Identification of an amino acid sequence in laminin mediating cell attachment, chemotaxis and receptor binding. *Cell* 48:989–996, 1987
20. Fuller SD, von Bonsdorff CH, Simons KH: Vesicular stomatitis virus infects and matures only through the basolateral surface of the polarized epithelial cell line MDCK. *Cell* 38:65–77, 1984
21. Gabow PA: Autosomal dominant polycystic kidney disease, in *The Cystic Kidney*, edited by Gardner KD, Bernstein J, Dordrecht, Kluwer Academic Publisher, 1990, pp 295–326
22. Grantham JJ: Fluid secretion, cellular proliferation, and pathogenesis of renal epithelial cysts. *J Am Soc Nephrol* 3:1843–1857, 1993
23. International Polycystic Kidney Disease Consortium: Polycystic kidney disease: The complete structure of the *PKD1* gene and its protein. *Cell* 81:289–298, 1995
24. Carone FA, Nakamura S, Punyarit P, Kanwar YS, Nelson WJ: Sequential tubular cell and basement membrane changes in polycystic kidney disease. *J Am Soc Nephrol* 3:244–253, 1992
25. Frisch SM, Francis H: Disruption of epithelial cell-matrix interactions induces apoptosis. *J Cell Biol* 124:619–626, 1994
26. Tang MJ, Hu JJ, Lin HH, Chiu WT, Jiang ST: Collagen gel overlay induces apoptosis of polarized cells in cultures: Disoriented cell death. *Am J Physiol* 275:C921–C931, 1998
27. Zhang Z, Vuori K, Reed JC, Ruoslahti E: The $\alpha5\beta1$ integrin supports survival of cells on fibronectin and up-regulation Bcl-2 expression. *Proc Natl Acad Sci USA* 92:6161–6165, 1995
28. Scoot G, Cassidy L, Busacco A: Fibronectin suppresses apoptosis in normal human melanocyte through an integrin-dependent mechanism. *J Invest Dermatol* 108:147–153, 1997
29. Globus RK, Doty SB, Lull JC, Holmuhamedov E, Humphries MJ, Damsky CH: Fibronectin is a survival factor for differentiated osteoblasts. *J Cell Sci* 111:1385–1393, 1998
30. Ruoslahti E, Pierschbacher MD: New perspectives in cell adhesion: RGD and integrins. *Science* 238:491–493, 1987
31. Saleman E, Santoro SA, Keely PJ: Loss of MDCK cells a2b1 integrin expression results in reduced cyst formation, failure of hepatocyte growth factor/scatter factor-induced branching morphogenesis, and increased apoptosis. *J Cell Sci* 108:3531–3540, 1995
32. Schoenenberger CA, Zuk A, Zinkl GM, Kendall D, Matlin KS: Integrin expression and localization in normal MDCK cell and transformed MDCK cells lacking apical polarity. *J Cell Sci* 107:527–541, 1994